

# SciSpot: Scientific Computing On Temporally Constrained Cloud Preemptible VMs

JCS Kadupitiya, Vikram Jadhao, Prateek Sharma

---

**Abstract**—Scientific computing applications are being increasingly deployed on cloud computing platforms. Transient servers such as EC2 spot instances and Google Preemptible VMs, can be used to lower the costs of running applications on the cloud by up to  $10\times$ . However, the frequent preemptions and resource heterogeneity of these transient servers introduces many challenges in their effective and efficient use. In this paper, we develop techniques for modeling and mitigating preemptions of transient servers, and present SciSpot, a software framework that enables low-cost scientific computing on the cloud. SciSpot deploys applications on Google Cloud Preemptible Virtual Machines that exhibit temporally constrained preemptions: VMs are always preempted in a 24 hour interval. Our empirical analysis shows that the preemption rate is bath-tub shaped, which raises multiple fundamental challenges in performance modeling and policy design. We develop a new reliability model for temporally constrained preemptions, and use statistical mechanics to show why the bath-tub shape is a fundamental characteristic.

SciSpot's design is guided by our observation that many scientific computing applications (such as simulations) are deployed as “bag” of jobs, which represent multiple instantiations of the same computation with different physical and computational parameters. For a bag of jobs, SciSpot finds the optimal transient server on-the-fly, by taking into account the price, performance, and preemption rates of different servers. SciSpot reduces costs by  $5\times$  compared to conventional cloud deployments, and reduces makespans by up to  $10\times$  compared to conventional high performance computing clusters.

## 1 INTRODUCTION

**Scientific Computing On Transient VMs.** Increasingly, cloud computing platforms have begun to supplement and complement conventional HPC infrastructure to meet the large computing and storage requirements of scientific applications. Public cloud platforms such as Amazon’s EC2, Google Cloud Platform, and Microsoft Azure, offer multiple benefits such as *on-demand* resource allocation, convenient pay-as-you-go pricing models, ease of provisioning and deployment, and near-instantaneous elastic scaling. However, the flexibility offered by cloud platforms comes at a literal cost: the price of deploying scientific computing applications can be significant, and continues to be a major hurdle towards adoption.

Conventionally, cloud VMs have been offered with “on-demand” availability, such that the lifetime of the VM is solely determined by the owner of the VM (i.e., the cloud customer). Increasingly however, cloud providers have begun offering low-cost VMs with *transient*, rather than continuous on-demand availability. Transient VMs can be unilaterally revoked and preempted by the cloud provider,

and applications running inside them face fail-stop failures. Due to their volatile nature, transient VMs are offered at steeply discounted rates. Amazon EC2 spot instances, Google Cloud Preemptible VMs, and Azure Batch VMs, are all examples of transient VMs, and are offered at discounts ranging from 50 to 90%.

However, deploying applications on cloud platforms presents multiple challenges due to the *fundamental* differences with conventional HPC clusters—which most applications still assume as their default execution environment. While the on-demand resource provisioning and pay-as-you-go pricing makes it easy to spin-up computing clusters in the cloud, the deployment of applications must be cognizant of the heterogeneity in VM sizes, pricing, and VM availability. Crucially, optimizing for *cost* in addition to makespan, becomes an important objective in cloud deployments. Furthermore, although using transient resources can drastically reduce computing costs, their preemptible nature results in frequent job failures. Preemptions can be mitigated with additional fault-tolerance mechanisms and policies [57], [51], although they impose additional performance and deployment overheads.

**Transient Computing Challenges.** To expand the usability and appeal of transient VMs, many systems and techniques have been proposed that seek to ameliorate the effects of preemptions and reduce the computing costs of applications. Fault-tolerance mechanisms [60], [51], resource management policies [59], [76], and cost optimization techniques [27], [61] have been proposed for a wide range of applications—ranging from interactive web services, distributed data processing, parallel computing, etc. These techniques have been shown to minimize the performance-degradation and downtimes due to preemptions, and reduce computing costs by up to 90%.

However, the success of these techniques depends on probabilistic estimates of when and how frequently preemptions occur. For instance, many fault-tolerance and resource optimization policies are parametrized by the mean time to failure (MTTF) of the transient VMs. A commonly used technique in transient computing is to periodically checkpoint application state, and the “optimal” checkpointing frequency that minimizes the total expected running time of a job depends on the MTTF of the VMs [25].

**Challenges with Google Preemptible VMs.** *Spot* markets (used by Amazon EC2’s spot instances and others) are a popular model, where preemptions are governed by dynamic

prices (which are in turn set using a continuous second-price auction [17]). In this paper, we focus on a different transient availability model—temporally constrained preemptions, which are found in Google Preemptible VMs. In this model, transient VMs have a fixed maximum lifetime, that acts as a temporal constraint on the preemption events. Google’s Preemptible VMs are temporally constrained—they have a maximum lifetime of 24 hours, and are always preempted within the  $[0, 24]$  hour interval.

The **temporally constrained preemption** model is distinct from spot markets, and presents fundamental challenges in preemption modeling and effective use of transient VMs. Transiency-mitigation techniques such as VM migration [60], checkpointing [57], [51], diversification [59], *all* use price-signals to model the availability and preemption rates of spot instances. With flat pricing, these approaches are not applicable. Furthermore, no other information about preemption characteristics is publicly available, not even coarse-grained metrics. To address this, we develop an *empirical* approach for understanding and modeling preemptions. We conduct a large empirical study of over 800 preemptions of Google Preemptible VMs, and develop an analytical probability model for temporally constrained preemptions.

Due to the temporal constraint on preemptions, classical models that form the basis of preemption modeling and policies, such as memoryless exponential failure rates, are not applicable. We find that preemption rates are *not* uniform, but bathtub shaped with multiple distinct temporal phases, and are incapable of being modeled by existing bathtub distributions such as Weibull. We capture these characteristics by **developing a new probability model**. Our model uses reliability theory principles to capture the 24-hour lifetime of VMs, and generalizes to VMs of different resource capacities, geographical regions, and across different temporal domains. Using our probability model, we find that bathtub failures can reduce the recomputation overhead of preemptions by more than  $10\times$  compared to uniform failures—which has important implications for cloud users and providers.

We show the applicability and effectiveness of our model by developing **optimized policies for job scheduling and checkpointing**. These policies are fundamentally dependent on empirical and analytical insights from our model. Our job-scheduling policy uses the bathtub behavior to decide whether to run a new job on a running VM or to request a new VM, and reduces job-failure probability by  $2\times$  compared to conventional memoryless policies. The bathtub distribution also requires a new approach to periodic checkpointing—since existing Young-Daly [25] checkpointing is restricted to memoryless preemptions. Our checkpointing policy combines our preemption model and dynamic programming to reduce the checkpointing overhead by more than  $5\times$ . These optimized policies act as building blocks for transient computing systems and for reducing the performance degradation and costs of preemptible VMs.

We implement and evaluate these policies as part of a batch computing service, **SciSpot**, which we also use for empirically evaluating the effectiveness of our model and policies under real-world conditions. SciSpot abstracts typical scientific computing workloads and workflows into a new unit of execution, which we call as a “bag of jobs”. These bags of jobs, ubiquitous in scientific computing, represent

multiple instantiations of the same application launched with possibly different physical and computational parameters. The bag of jobs is especially useful for machine-learning integrated scientific computing applications, in which the same application is run with different parameters to curate “training data sets” for surrogates [] of physical systems. The bag of jobs abstraction permits efficient implementation of our optimized policies, and allows SciSpot to lower the costs and barriers of transient VMs for scientific computing applications.

Towards our goal of harnessing temporally constrained transient VMs for modern scientific computing workloads, we make the following contributions:

- 1) We conduct a large-scale, first of its kind empirical study of preemptions of Google’s Preemptible VMs<sup>1</sup>. We then show a statistical analysis of preemptions based on the VM type, temporal effects, geographical regions, etc. Our analysis indicates that the 24-hour constraint is a defining characteristic, and that the preemption rates are *not* uniform, but have distinct phases.
- 2) We develop a probability model of constrained preemptions based on empirical and statistical insights that point to distinct failure processes underpinning the preemption rates. Our model captures the key effects resulting from the 24 hour lifetime constraint associated with these VMs, and we analyze it through the lens of reliability theory.
- 3) Based on our preemption model, we develop optimized policies for job scheduling and checkpointing that minimize the total time and cost of running applications. These policies reduce job running times by up to  $2\times$  compared to existing preemption models used for transient VMs.
- 4) We implement and evaluate our policies as part of a batch computing service for Google Preemptible VMs. SciSpot introduces the bag of jobs abstraction for scientific simulation applications, and can reduce computing costs by  $5\times$  compared to conventional cloud deployments, and reduce the performance overhead of preemptible VMs to less than 3%.

## 2 BACKGROUND

We now give an overview of transient cloud computing, and the use of preemption models in transient computing systems.

### 2.1 Transient Cloud Computing

Infrastructure as a service (IaaS) clouds such as Amazon EC2, Google Public Cloud, Microsoft Azure, etc., typically provide computational resources in the form of virtual machines (VMs), on which users can deploy their applications. Conventionally, these VMs are leased on an “on-demand” basis: cloud customers can start up a VM when needed, and the cloud platform provisions and runs these VMs until they are shut-down by the customer. Cloud workloads, and hence the utilization of cloud platforms, shows large temporal variation. To satisfy user demand, cloud capacity is typically provisioned for the *peak* load, and thus the average utilization tends to be low, of the order of 25% [73], [23].

<sup>1</sup> Preemption dataset available at <https://github.com/kadupitiya/goog-preemption-data/>

To increase their overall utilization, large cloud operators have begun to offer their surplus resources as low-cost servers<sup>2</sup> with *transient* availability, which can be preempted by the cloud operator at any time (after a small advance warning). These preemptible servers, such as Amazon Spot instances [2], Google Preemptible VMs [5], and Azure batch VMs [13], have become popular in recent years due to their discounted prices, which can be 7-10× lower than conventional non-preemptible servers. Due to their popularity among users, smaller cloud providers such as Packet [6] and Alibaba [1] have also started offering transient cloud servers.

However, effective use of transient servers is challenging for applications because of their uncertain availability [64]. Preemptions are akin to fail-stop failures, and result in loss of the application memory and disk state, leading to downtimes for interactive applications such as web services, and poor throughput for batch-computing applications. Consequently, researchers have explored fault-tolerance techniques such as checkpointing [57], [51], [67] and resource management techniques [59] to ameliorate the effects of preemptions. The effect of preemptions depends on the application’s delay insensitivity and fault model, and mitigating preemptions for different applications remains an active research area [41].

## 2.2 Modeling Preemptions of Transient VMs

Underlying *all* techniques and systems in transient computing is the notion of using some probabilistic or even a deterministic model of preemptions. Such a preemption model is then used to quantify and analyze the impact of preemptions on application performance and availability; and to design model-informed policies to minimize the effect of preemptions. For example, the preemption rate or MTTF (Mean Time To Failure) of transient servers has found extensive use in selecting the appropriate type of transient server for applications [59], [67], determining the optimal checkpointing frequency [57], [51], [34], [30], etc.

Preemptions of spot market based VMs (such as EC2 spot instances) are based on their *price*, which is dynamically adjusted based on the supply and demand of cloud resources. Spot prices are based on a continuous second-price auction, and if the spot price increases above a pre-specified maximum-price, then the server may be preempted [17]. Thus, the time-series of these spot prices can be used for understanding preemption characteristics such as the frequency of preemptions and the “Mean Time To Failure” (MTTF) of the spot instances. Publicly available [39] historical spot prices have been used to characterize and model spot instance preemptions [60], [85], [62], [77]. For example, past work has analyzed spot prices and shown that the MTTFs of spot instances of different hardware configurations and geographical zones range from a few hours to a few days [78], [54], [77], [16], [79]. Spot instance preemptions can be modeled using *memoryless* exponential distributions [85], [58], [57], [30], [83], which permits optimized periodic checkpointing policies such as Young-Daly [25].

However, using pricing information for preemption modeling is *not* a generalizable approach, and is not applicable to models of transient availability used by other transient VMs like Google Preemptible VMs and Azure Low-priority batch

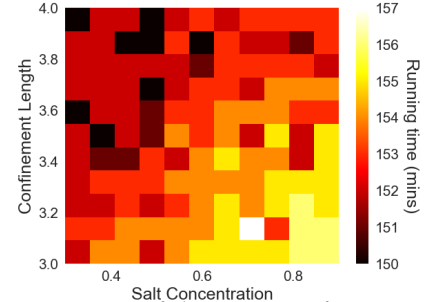


Fig. 1: Running times of the Nanoconfinement application with different sets of parameters have low variation.

VMs. These VMs have *flat* pricing, and thus pricing cannot be used to infer preemptions. Moreover, these cloud providers (Google and Azure) do not expose *any* public information about their preemption characteristics, even metrics like MTTF that can be useful in mitigating preemptions [83]. In this paper, we propose an empirical approach for modeling preemptions of temporally constrained VMs such as Google Preemptible VMs. Our empirical data and the resulting preemption model allows the development of preemption mitigation policies. Google Preemptible VMs have a maximum lifetime of 24 hours, and this *constrained* preemption is not *memoryless*, and requires new fundamental modeling approaches.

## 2.3 Scientific Simulation Workloads

The typical workflow associated with most scientific computing applications, often involves evaluating a computational model across a wide range of physical and computational parameters. For instance, constructing and calibrating a molecular dynamics application (such as Nanoconfinement [?]), usually involves running a simulation with different physical parameters such as characteristic sizes and interaction potentials, as well as computational parameters such as simulation timesteps. Each of these parameters can take a wide range of values, resulting in a large number of combinations which must be evaluated by invoking the application multiple times (also known as a parameter sweep). Since each computational job explores a single combination of parameters, this results in executing a “bag of jobs”, with each job in the bag running the same application, but with possibly different parameters.

The bag of jobs execution model is pervasive in scientific computing and applicable in many contexts. In addition to exploratory parameter sweeps, bags of jobs also result from running the application a large number of times to account for the model or computational stochasticity, and can be used to obtain tighter confidence intervals. Increasingly, bags of jobs also arise in the emerging research that combines statistical machine learning (ML) techniques and scientific simulations [14], [20], [56]. For instance, large bags of jobs are run to provide the necessary training and testing data for learning statistical models (such as neural networks) that are then used to improve the efficacy of the simulations [?].

Bags of jobs are analogous to, but distinct from the bag of *tasks* design [22], where applications are decomposed into independent processes to enable flexible task scheduling. In contrast, the bags of jobs abstraction is independent of the application design—a bag of jobs may consist of a synchronous MPI program that is not amenable to flexible scheduling.

2. We use servers and VMs interchangeably throughout the paper.

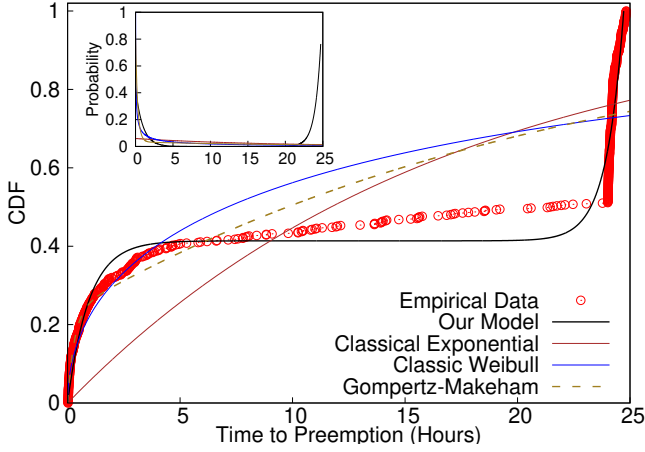


Fig. 2: CDF of lifetimes of Google Preemptible VMs. Our proposed distribution for modeling the constrained preemption dynamics provides a better fit to the empirical data compared to other failure distributions. Inset shows the probability density functions.

The bag of jobs execution model has multiple characteristics, that give rise to unique challenges and opportunities when deploying them on transient cloud servers. Since bags of jobs require a large amount of computing resources, deploying them on the cloud can result in high overall costs, thus requiring policies for minimizing the cost and overall running time. The similarity in execution characteristics of jobs (such as their running times and parallel speedup) allows for bag-wide optimizations (Figure 1). And last, treating entire bags of jobs as an execution unit, instead of individual jobs, can allow us to use partial redundancy between jobs and reduce the fault-tolerance overhead to mitigate transient server preemptions.

### 3 PREEMPTION ANALYSIS AND MODELING OF GOOGLE PREEMPTIBLE VMs

In our quest to understand temporally constrained preemptions, we conduct an empirical study of preemptions of Google Preemptible VMs. Based on our observations and insights from the study, we then develop a probability model for temporally constrained preemptions, which we then provide a statistical mechanics interpretation for.

#### 3.1 Empirical Study Of Preemptions

**Methodology.** We launched 870 Google Preemptible VMs of different types over a two month period (Feb–April 2019), and measured their time to preemption (i.e., their useful lifetime). VMs of different resource capacities were launched in four geographical regions; during days and nights and all days of the week; and running different workloads<sup>3</sup>. We launched VMs in their default resource configurations (CPU and memory), and do not use custom VM sizes. To ensure the generality of our empirical observations, VMs were not launched during well-known peak utilization days (such as Black Friday). The preemption data collection was bootstrapped: a small amount of data points were used to estimate and model the preemption CDF, which we then

used to run our batch computing service (described and evaluated in Sections 5 and 6), which generated the rest of the preemption data. Due to the relatively high preemption rates compared to EC2 spot instances, we were able to collect these data points for less than \$5,000.

A sample of over 100 such preemption events are shown in Figure 2, which shows cumulative distribution function (CDF) of the lifetime of the n1-highcpu-16 VMs in the us-east1-b zone. Empirically, our main observation is: *The lifetimes of VMs are not uniformly distributed, but have three distinct phases.* In the first (initial) phase, characterized by VM lifetime  $t \in [0, 3]$  hours, we observe that many VMs are quickly preempted after they are launched, and thus have a steep rate of failure. The rate of failure (preemption rate) is the derivative of the CDF. The early high rate of failure reflects that the cloud service provider takes into account VM lifet ime in prioritizing preempting “younger” VMs, in other words, the number of simultaneous VMs launched does have an effect on their failure rate. In the second phase, VMs that survive past 3 hours enjoy a relatively low preemption rate over a relatively broad range of lifetime (characterized by the slowly rising CDF in Figure 2). The third and final phase exhibits a steep increase in the number of preemptions as the preemption deadline of 24 hours approaches. The overall rate of preemptions is “bathtub” shaped as shown by the solid black line in the inset of Figure 2.

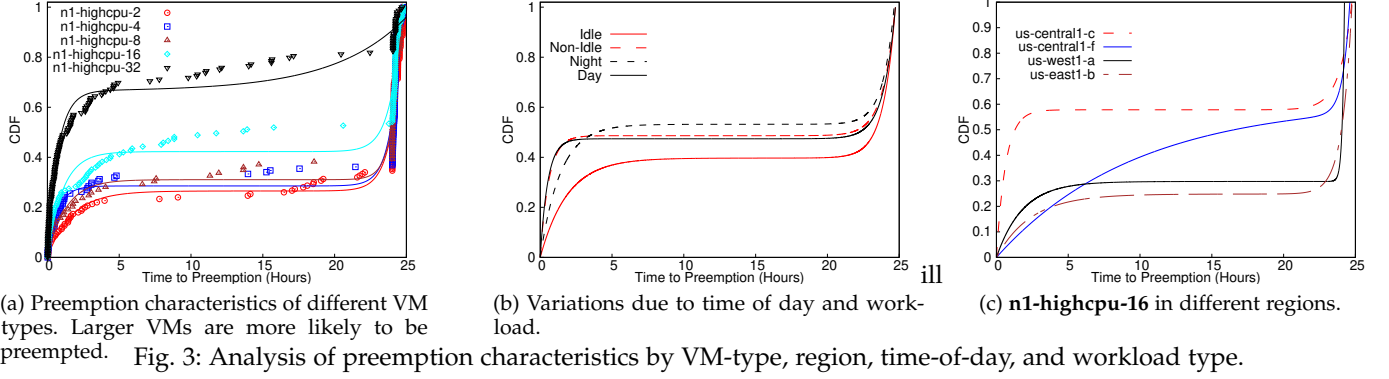
**Observation 1:** *The lifetimes of VMs are not uniformly distributed, but have three distinct phases.*

In the first (initial) phase, characterized by VM lifetime  $t \in [0, 3]$  hours, we observe that many VMs are quickly preempted after they are launched, and thus have a steep rate of failure. The rate of failure (preemption rate) is the derivative of the CDF. The early high rate of failure reflects that the cloud service provider takes into account VM lifet ime in prioritizing preempting “younger” VMs, in other words, the number of simultaneous VMs launched does have an effect on their failure rate. In the second phase, VMs that survive past 3 hours enjoy a relatively low preemption rate over a relatively broad range of lifetime (characterized by the slowly rising CDF in Figure 2). The third and final phase exhibits a steep increase in the number of preemptions as the preemption deadline of 24 hours approaches. The overall rate of preemptions is “bathtub” shaped as shown by the solid black line in the inset of Figure 2 (discussed in detail below).

**Observation 2:** *The preemption behavior, imposed by the constraint of the 24 hour lifetime, is substantially different from conventional failure characteristics of hardware components and EC2 spot instances.*

In “classical” reliability analysis, the rate of failure usually follows an exponential distribution  $f(t) = \lambda e^{-\lambda t}$ , where  $\lambda = 1/\text{MTTF}$ . Figure 2 shows the CDF ( $= 1 - e^{-\lambda t}$ ) of the exponential distribution when fitted to the observed preemption data, by finding the distribution parameter  $\lambda$  that minimizes the least squares error. The classic exponential distribution is unable to model the observed preemption behavior because it assumes that the rate of preemptions is independent of the lifetime of the VMs, i.e., the preemptions

3. Preemption rates can also be affected by number of VMs launched simultaneously, which we limited to between 1 and 10.



(a) Preemption characteristics of different VM types. Larger VMs are more likely to be preempted. Fig. 3: Analysis of preemption characteristics by VM-type, region, time-of-day, and workload type.

(b) Variations due to time of day and workload.

(c) n1-highcpu-16 in different regions.

are *memoryless*. This assumption breaks down when there is a fixed upper bound on the lifetime.

**Observation 3:** *The three preemption phases and associated bathtub shaped preemption probability are general, universal characteristics of Preemptible VMs.*

Our empirical study looked at preemptions of VMs of different sizes (Figure 3a), at different times of the day (Figure 3b), in different geographical zones (Figure 3c), and running different workloads. In all cases, we find that there are three distinct phases associated with the preemption dynamics giving rise to the bathtub shaped preemption probability.

**Observation 4:** *Larger VMs have a higher rate of preemptions.*

Figure 3a shows the preemption data from five different types of VMs in the Google Cloud n1-highcpu-{2, 4, 8, 16, 32}, where the number indicates the number of CPUs. All VMs are running in the us-central1-c zone. We see that the larger VMs (16 and 32 CPUs) have a higher probability of preemptions compared to the smaller VMs. While this could be simply due to higher demand for larger VMs, it can also be explained from a cluster management perspective. Larger VMs require more computational resources (such as CPU and memory), and when the supply of resources is low, the cloud operator can quickly reclaim a large amount of resources by preempting larger VMs. This observed behavior aligns with the guidelines for using preemptible VMs that suggests the use of smaller VMs when possible [5].

**Observation 5:** *Preemptions exhibit diurnal variations, and are also affected by the workload inside the VM.*

From Figure 3b, we can see that VMs have a slightly longer lifetime during the night (8 PM to 8 AM) than during the day<sup>4</sup>. This is expected because fundamentally, the preemption rates are higher during periods of higher demand. We also notice that completely idle VMs have longer lifetimes than VMs running some workload. Presumably, this could be a result of the lower resource utilization of idle VMs being more amenable to resource overcommitment, and result in lower preemptions.

**Significance of bathtub preemptions.** The bathtub shaped preemption distribution is not a coincidence. It is a result of fundamental characteristics of constrained preemptions that benefit applications. For applications that do not incorporate explicit fault-tolerance (such as checkpointing), early preemptions result in less wasted work than if the preemptions were

uniformly distributed over the 24 hour interval. Furthermore, the low rate of preemptions in the middle periods allows jobs that are smaller than 24 hours to finish execution with only a low probability of failure, once they survive the initial preemption phase. We compare application performance with bathtub preemptions and uniformly distributed preemptions later in Section 6, and find that bathtub preemptions can reduce the performance overheads of preemptions by up to 10×. However, effective policies for constrained preemptions requires a probability model of preemptions, which must incorporate the temporal constraint and the steep bathtub behavior. Existing preemption models are not applicable, and we present our new model next.

### 3.2 Failure Probability Model

We now develop an analytical probability model for finding a preemption at a given time that is faithful to the empirically observed data and provides a basis for developing running-time and cost-minimizing optimizations. Modeling the dynamics of preemptions constrained by a finite deadline raises many challenges for existing preemption models that have been used for other transient servers such as EC2 spot instances. We first discuss why existing approaches to preemption modeling are not adequate, and then present our probability model and associated reliability theory connections.

#### 3.2.1 Our model

Our failure probability model seeks to address the drawbacks of existing reliability theory models for modeling constrained preemptions. The presence of three distinct phases exhibiting non-differentiable transition points (sudden changes in CDF near the deadline, for example) suggests that for accurate results, models that treat the probability as a step function (CDF as a piecewise-continuous function) could be employed. However, this limits the range of model applicability and general interpretability of the underlying preemption behavior. Our goal is to provide a broadly applicable, continuously differentiable, and informative model built on reasonable assumptions.

We begin by making a key assumption: the preemption behavior arises from the presence of *two* distinct failure processes. The first process dominates over the initial temporal phase and yields the classic exponential distribution that captures the high rate of early preemptions. The second process dominates over the final phase near the 24 hour maximum VM lifetime and is assumed to be characterized

4. Time-zone local to the VM's location.

by an exponential term that captures the sharp rise in preemptions that results from this constrained lifetime.

Based on these observations, we propose the following general form for the CDF:

$$\mathcal{F}(t) = A \left( 1 - e^{-\frac{t}{\tau_1}} + e^{\frac{t-b}{\tau_2}} \right) \quad (1)$$

where  $t$  is the time to preemption,  $1/\tau_1$  is the rate of preemptions in the initial phase,  $1/\tau_2$  is the rate of preemptions in the final phase,  $b$  denotes the time that characterizes “activation” of the final phase where preemptions occur at a very high rate, and  $A$  is a scaling constant. The model is fit to data for  $0 < t < L$ , where  $L \approx 24$  hours represents the temporal interval (deadline). Combination of the 4 fit parameters ( $\tau_1, \tau_2, b$ , and  $A$ ) are chosen to ensure that boundary condition  $\mathcal{F}(0) \approx 0$  is satisfied. In practice, typical fit values yield  $b \approx 24$  hours,  $\tau_1 \in [0.5, 1, 5]$ ,  $\tau_2 \approx 0.8$ , and  $A \in [0.4, 0.5]$ .

For most of its life, a VM sees failures according to the classic exponential distribution with failure-rate equal to  $1/\tau_1$  – this behavior is captured by the  $1-e^{-t/\tau_1}$  term in Equation 1. As VMs get closer to their maximum lifetime imposed by the cloud operator, they are reclaimed (i.e., preempted) at a high rate  $1/\tau_2$ , which is captured by the second exponential term,  $e^{(t-b)/\tau_2}$  of Equation 1. Shifting the argument ( $t$ ) of this term by  $b$  ensures that the exponential reclamation is only applicable near the end of the VM’s maximum lifetime and does not dominate over the entire temporal range.

The analytical model and the associated distribution function  $\mathcal{F}$  introduced above provides a much better fit to the empirical data (Figure 2) compared to other models, and captures the different phases of the preemption dynamics through parameters  $\tau_1, \tau_2, b$ , and  $A$ . These parameters can be obtained for a given empirical CDF using least squares function fitting methods (we use scipy’s `optimize.curve_fit` with the dogbox technique [7]). The failure or preemption rate can be derived from the CDF in Equation 1 as:

$$f(t) = \frac{d\mathcal{F}(t)}{dt} = A \left( \frac{1}{\tau_1} e^{-t/\tau_1} + \frac{1}{\tau_2} e^{\frac{t-b}{\tau_2}} \right). \quad (2)$$

$f(t)$  vs.  $t$  yields a bathtub type failure rate function for the associated fit parameters (inset of Figure 2).

In the absence of any prior work on constrained preemption dynamics, our aim is to provide an interpretable model with a minimal number of parameters, that provides a sufficiently accurate characterization of features present in the preemption data. Extension of this model to include more failure processes would introduce more parameters and reduce the generalization power. Further, this model as well as the optimization policies derived from it offer pathways to quantify additional effects arising due to the inclusion of more failure processes.

### 3.2.2 Reliability Analysis

We now analyze and place our model in a reliability theory framework.

**Expected Lifetime:** Our analytical model helps crystallize the differences in VM preemption dynamics, by allowing us

to easily calculate their expected lifetime. More formally, we define the expected lifetime of a VM ( $\mathcal{L}$ ) as:

$$E[\mathcal{L}] = \int_0^L t f(t) dt = -A(t+\tau_1)e^{-t/\tau_1} + A(t-\tau_2)e^{\frac{t-b}{\tau_2}} \Big|_0^L \quad (3)$$

where  $f(t)$  is the rate of preemptions of the VM (Equation 2). This expected lifetime can be used in lieu of MTTF, for policies and applications that require a “coarse-grained” comparison of the preemption rates of servers of different types, which has been used for cost-minimizing server selection [57].

**Hazard Rate:** The hazard rate  $\lambda(t)$  governs the dynamics of the failure (or survival) processes. It is generally defined as  $\lambda(t) = \frac{f(t)}{S(t)}$  and often expressed via the following differential equation (rate law):

$$\frac{dS(t)}{dt} = -\lambda(t)S(t), \quad (4)$$

where  $S(t) = 1 - F(t)$  is the survival function associated with a CDF  $F(t)$ , and  $f(t) = dF(t)/dt$  is the failure probability function (rate) at time  $t$ . The survival function indicates the amount of VMs that have survived at time  $t$ . The hazard rate can also be directly expressed in terms of the CDF as follows:  $1 - F(t) = \exp \int_0^t -\lambda(x) dx$ . The exponential distribution has a constant hazard rate  $\lambda$ . The Gompertz-Makeham distribution has an increasing failure rate to account for the increase in mortality, and its hazard rate is accordingly time-dependent and given by  $\lambda(t) = \lambda + \alpha e^{\beta t}$ .

Since we model multiple failure rates and deadline-induced preemptions, our hazard rate is expected to increase with time. Defining the survival function for our model:  $S = 1 - \mathcal{F}$ , and using Eq. 4 yields the hazard rate associated with our model:

$$\lambda = \frac{r_1 e^{-r_1 t} + r_2 e^{r_2(t-b)}}{1/A - 1 + e^{-r_1 t} - e^{r_2(t-b)}} \quad (5)$$

where we have introduced  $r_1 = 1/\tau_1$ ,  $r_2 = 1/\tau_2$  to denote the rates of preemptions associated with initial and final phases respectively.

Recall that the sharp increase in preemption rate only happens close to the deadline, which means that  $b \lesssim L$ . Thus, when  $0 < t \ll b$ , we get  $\lambda(t) \approx r_1$ , mimicking the hazard rate for the classic exponential distribution. As  $t$  approaches and exceeds  $b$  (i.e.,  $b \lesssim t < L$ ), the increase in the hazard rate due to the second failure process kicks in, accounting for the deadline-induced rise in preemptions. Note that our hazard rate satisfies  $\lambda(t) \geq 0$  for  $0 < t < L$ .

### 3.3 Statistical mechanics of constrained preemptions

For constrained preemptions, one might expect to see uniformly distributed preemptions with a probability  $1/L$  over  $[0, L]$ . However, as our empirical analysis shows, the preemption distribution is bathtub-shaped. Interestingly, we can show using exact analytical arguments that non-uniform, bathtub distributions are in fact a *general* characteristic of systems with constrained preemptions, modulo some assumptions.

**Lemma 1.** Consider  $N$  randomly distributed preemptions over an interval  $[0, L]$ . Assume that each preemption takes  $w > 0$

time-units to perform, and preemptions cannot overlap, i.e., they occur in a mutually exclusive manner. Then, there exists  $\epsilon > 0$  such that  $P(L - \epsilon) > \frac{1}{L}$ , where  $P(t)$  is the probability of finding a preemption at time  $t$ .

*Proof.* We first make some preliminary remarks and introduce concepts necessary to complete the proof.

Firstly, mutual exclusion of preemptions implies that there is a finite non-zero waiting time  $w > 0$  between preemptions. For  $N$  preemptions to occur within  $L$  interval, evidently, we must have  $Nw < L$ . Also, while  $w > 0$ , the time to perform the preemption is generally expected to be much smaller than the total time interval  $L$  (i.e.,  $w \ll L$ ).  $N$  preemptions occupy a “temporal volume” of  $Nw$  (volume here represents the one-dimensional volume). We assume that while a preemption may start at  $t = 0$ , the last preemption must finish by  $t = L$ . Thus, the amount of free or excluded “temporal volume” available within the constrained system is  $L_e = L - w - (N-1)w = L - Nw$ . The concept of excluded volume arising due to the finite-size of the particles is central to understand the physics of material systems in confined environments and is explain the origin of steric forces and correlations [49], [40], [65].

Secondly, we note that the system of  $N$  preemptions within a constrained deadline of interval  $L$  maps *exactly* to a well known and analytically solvable system in classical statistical mechanics, the one-dimensional Tonks gas model [71]. The Tonks gas model describes a system of  $N$  non-overlapping particles of finite size  $w$  that are constrained to move within a line segment of length  $L$ . The structural quantities associated with this system, including the probability of finding a particle at position  $x$  within the spatial confinement of length  $L$ , are computed by evaluating the partition function of the system, which essentially measures the number of valid system configurations [49]. Employing this mapping, we consider a system of  $N$  non-overlapping preemptions constrained within a “time confinement” of size  $L$ . Each preemption has access to an excluded volume of  $L_e$  within this constrained system. The number of ways in which  $N$  preemptions can occur within the interval  $L$  is equivalent to the number of valid configurations for this system which is given by its partition function:  $Z_N = L_e^N = (L - Nw)^N$ .

We are interested in calculating the probability that a preemption starts at time  $t = L - w$ , i.e.,  $P(L - w)$ . Given  $w \ll L$ ,  $P(L - w)$  is the probability of finding a preemption near the deadline. The assumption of mutually exclusive preemptions implies that no other preemption can be found for  $t > L - w$ , that is,  $P(t > L - w) = 0$ . Hence, the remaining  $N - 1$  preemptions must occur such that the last of those finish by  $t = L - w$ . In other words, the preemption at time  $L - w$  essentially sets an effective deadline for the other  $N - 1$  preemptions. The number of ways those  $N - 1$  preemptions can happen within the time interval of  $L - w$  is given by the partition function  $Z_{N-1} = L_e^{N-1} = (L - 2w - (N-2)w)^{N-1} = (L - Nw)^{N-1}$ , where  $L_e = L - Nw$  is the corresponding excluded temporal volume available to each of the  $N - 1$  preemptions. It is interesting to note that this excluded volume is the same as that of the original  $N$  preemption system: this fortuitous result arises because the decrease in the available volume (“time confinement”)

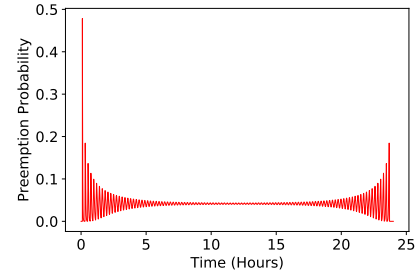


Fig. 4: Preemption probability computed using the partition function defined for a simple constrained system is also bathtub shaped.

to place the preemptions is commensurate with the need to place fewer ( $N - 1$ ) preemptions.

The probability  $P(L - w)$  is obtained as the ratio of the valid configurations given by the two partition functions computed above. That is,  $P(L - w) = Z_{N-1}/Z_N = \frac{1}{L - Nw} > \frac{1}{L}$ , since  $N \geq 1$  and  $w > 0$ . Choosing  $\epsilon = w > 0$  completes the proof.  $\square$

By symmetry arguments, the above lemma is in fact valid for both the end points of the interval, i.e.,  $P(\epsilon) > \frac{1}{L}$ . In other words, the probability of preemption is higher near the end points (deadline) than the average preemption probability of  $1/L$ , and we get a bathtub shaped distribution. For the above proof, we assumed that each preemption event occurs over a timespan of  $w$ , which is determined by the preemption warning that the cloud platform provides (which is 30 seconds for Google Preemptible VMs and 120 seconds for Amazon EC2 spot instances). Preempting a VM and reclaiming its resources involves manipulating the cluster-management state, and mutually exclusive preemptions may be convenient for cluster management, since serializing VM preemptions makes accounting and other cluster operations easier. From an application standpoint, non-overlapping preemptions are also beneficial, since handling multiple concurrent preemptions is significantly more challenging [59].

Thus, statistical mechanics indicates that the bathtub distribution follows from the constrained and non-overlapping nature of preemptions, if we assume no other external factors or cloud policies influencing the preemptions. To validate this, we conduct a monte carlo simulation of temporally constrained and non-overlapping preemptions. Figure ?? shows that the preemption probability using this first-principles approach *also* follows the bathtub shape that is found in the empirical data.

#### 4 POLICIES FOR AMELIORATING CONSTRAINED PREEMPTIONS

Having analyzed the statistical behavior of constrained preemptions and presented our probability model, we now examine how the bathtub shape of the failure rate impacts applications. Based on insights drawn from our statistical analysis and the model, we develop various policies for ameliorating the effects of preemptions. Prior work in transient computing has established the benefits of such policies for a broad range of applications. However, the constrained nature of preemptions introduces new challenges that do

not arise in other transient computing environments such as Amazon EC2 spot instances, and thus new approaches are required. In this section, we first analyze the impact of constrained preemptions on job running time, and then develop new constrained-preemption aware policies for job scheduling and checkpointing. We will focus on long-running batch jobs that arise in many applications such as scientific computing. Extensions of our models and policies to distributed applications with different failure semantics is part of our future work.

#### 4.1 Job Running Time Modeling

SciSpot uses our bathtub probability model to predict the total running time (i.e., the makespan) of the job. When a preemption occurs during the job's execution, it results in wasted work, assuming there is no checkpointing. This increases the job's total expected running time, since it must restart after a preemption. The expected wasted work depends on two factors:

- 1) The probability of the job being preempted during its execution.
- 2) When the preemption occurs during the execution.

We can analyze the wasted work due to a preemption using the failure probability model. We first compute the expected amount of wasted work *assuming* the job faces a single preemption, which we denote by  $E[W_1(T)]$ , where  $T$  is the original job running time (without preemptions):

$$E[W_1(T)] = \int_0^T t P(t|t \leq T) dt. \quad (6)$$

Here,  $P(t|t \leq T) = P(t)/P(t \leq T)$ .  $P(t \leq T)$  is the probability that there is a preemption within time  $T$  and is given by  $P(t \leq T) = F(T)$ , where  $F(T)$  is the CDF (Equation 1).  $P(t)$  is the probability of a preemption at time  $t$ , and is given by  $P(t) = f(t)$ , where  $f(t)$  is the preemption rate (Equation 2). We can therefore write the above equation as:

$$E[W_1(T)] = \int_0^T t P(t|t \leq T) dt = \frac{1}{F(T)} \int_0^T t f(t) dt. \quad (7)$$

We note that the integral is the same as the "expected lifetime", given by Equation 3. The above expression for the expected waste given a single preemption can be used by users and application frameworks to estimate the increase in running time due to preemptions. The total running time (also known as makespan) of a job *with* preemptions is given by:

$$E[T] = P(\text{no failure}) T + P(1 \text{ failure}) (T + E[W_1(T)]), \quad (8)$$

where  $P(\text{no failure}) = P(t > T) = 1 - F(T)$  and  $P(1 \text{ failure}) = P(t \leq T) = F(T)$ . Expanding out these terms and using Equation 7, we get

$$\begin{aligned} E[T] &= (1 - F(T)) T + F(T) (T + E[W_1(T)]) \\ &= T + \int_0^T t f(t) dt. \end{aligned} \quad (9)$$

This expression for the expected running time assumes that the job will be preempted at most once. An expression which considers multiple ( $> 1$ ) job failures easily follows from this base case, but presents relatively low practical value.

**Consequences for applications:** Based on our analysis, both the increase in wasted time ( $E[W_1(T)]/T$ ) and expected running time ( $E[T]/T$ ) depend on the length of the job for non-memoryless constrained preemptions. For memoryless exponential distributions, the expected waste is simply  $T/2$ , but this assumption is not valid for constrained preemptions, and thus job lengths must be considered when evaluating the suitability of Preemptible VMs.

Users and transient computing systems can use the expected running time analysis for scheduling and monitoring purposes. Since the preemption characteristics are dependent on the type of the VM and temporal effects, this analysis also allows principled *selection* of VM types for jobs of a given length. For instance, VMs having a higher initial rate of preemptions are particularly detrimental for short jobs, because the jobs will see high rate of failure and are not long enough to run during the VM's stable period with low preemption rates. We evaluate the expected wasted time and running time for Google Preemptible VMs later in Section 6.

#### 4.2 Transition-Points based Job Scheduling and VM Reuse Policy

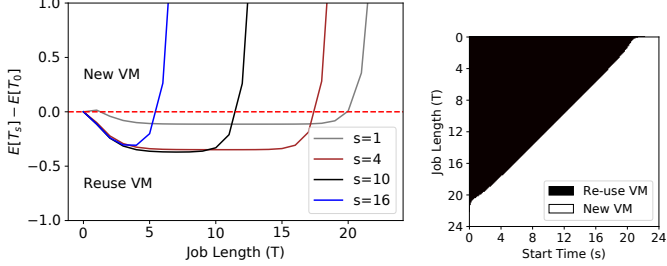
Our bathtub probability model also allows us to develop optimized job-scheduling policies for *reducing* job-failures in the bag of jobs execution model. In the case of deadline-constrained bathtub preemptions, we face a choice: we can either run a new job on an already running VM, or relinquish the VM and run the job on a *new* VM. This choice is important in the case of non-uniform failure rates, since the job's failure probability depends on the "age" of the VM. Because of the bathtub failure distribution, VMs enjoy a long period of low failure rates during the middle of their total lifespan. Thus, it is beneficial to *reuse* VMs for multiple jobs, and relinquishing VMs after every job completion may not be an optimal choice.

However, jobs launched towards the end of VM life face a tradeoff. While they may start during periods of low failure rate, the 24 hour deadline-imposed sharp increase in preemptions poses a high risk of preemptions, especially for longer jobs. The alternative is to discard the VM and run the job on a new VM. However, since newly launched VMs also have high preemption rates (and thus high job failure probability), the choice of running the job on an existing VM vs. a new VM is not obvious.

Our job scheduling policy uses the preemption model to determine the preemption probability of jobs of a given length  $T$ . Assume that the running VM's age (time since launch) is  $s$ . The intuition is to reuse the VM only if the expected running time is lower, compared to running on a new VM. To compute the expected running time of a job of length  $T$  starting at vm-age  $s$ , we modify our earlier expression for running time (Equation 9) to:

$$E[T_s] = T + \int_s^{s+T} t f(t) dt \quad (10)$$

The alternative is to discard the VM and launch a new VM, in which case the expected running time is  $E[T_0]$ . Our job-scheduling policy is simple: When a job of running time  $T$  attempts to start on a VM of age  $s$ , if  $E[T_s] \leq E[T_0]$ , then we run the job on the existing VM. Otherwise, a new VM is launched.



(a) Difference in expected running times. (b) Transition boundary.

Fig. 5: Reusing vs. running on a new VM.

**Transition Points Analysis.** SciSpot develops on the above insight and determines the job-scheduling and VM-reuse decision. Based on different job lengths within a bag of jobs and the age of the VM, we minimize the total expected running time of a job. For a given job running time ( $T$ ), and the VM age ( $s$ ), we can compute  $\delta(s, T) = E[T_s] - E[T]$ . If  $\delta(s, T) \geq 0$ , then a new VM is used, as illustrated in Figure 5a. The Figure shows that the reusing VMs is preferred for shorter job lengths, and the range of jobs for which for which reusing is good depends on the current age of the VM: younger VMs ( $s=1$ ) can be used for longer VMs compared to older VMs. For a given VM type, we precompute this function for different  $s, T$  values, and find the job length transition points where launching a new VM is suitable. The precomputed  $\delta(s, T)$  can be seen in Figure 5b. Using this figure, SciSpot, and users in general, can simply lookup the job and VM attributes, and determine the optimal decision.

#### 4.3 Cost-aware VM Selection

VM-selection is an important optimization in cloud environments, because VMs have different tradeoffs of cost, performance, and preemption characteristics. Application performance is affected by the size of the VM (due to network communication and parallel scaling overheads), and the preemption rates. We propose to develop cost models for selecting the “right” type of VMs that minimizes the expected job failure probability and cost by using the analytical preemption models. Our evaluation indicates that careful VM selection can reduce costs by up to 30%.

We assume that the total resource requirement for a job,  $\mathcal{R}$ , is provided by the user based on prior speedup data, the user’s cloud budget, and the deadline for job completion. Since server selection involves a tradeoff between cost, performance, and preemptions, we develop a model that allows us to optimize the resource allocation and pick the best VM type that minimizes the expected cost of running an application on SciSpot.

Let us assume that the cloud provider offers  $N$  server types, with the price (per unit time) of a server type equal to  $c_i$ . The overall expected cost of running a job can then be expressed as follows:

$$E[C_{(i,n_i)}] = n_i \times c_i \times E[\mathcal{T}_{(i,n_i)}]. \quad (11)$$

Here,  $E[\mathcal{T}_{(i,n_i)}]$  denotes the expected makespan of the job (accounting for preemptions) on  $n_i$  servers of type  $i$ . This turnaround time depends on whether the job needs to be recomputed because of preemptions, and is given by

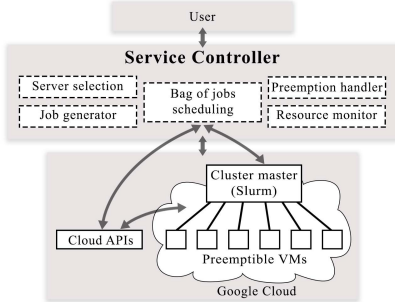


Fig. 6: Architecture and system components of SciSpot

Equation 9. SciSpot therefore searches over all available and acceptable VM types (modulo any resource constraints on minimum memory/CPU/GPUs), and picks the VM type which yields the lowest expected cost.

#### 5 SCI-SOTP DESIGN AND IMPLEMENTATION

We have implemented SciSpot as a prototype batch computing service that implements various policies for constrained preemptions. We use it to examine the effectiveness and practicality of our model and policies in real-world settings. SciSpot is implemented as a light-weight, extensible framework that makes it convenient and cheap to run batch jobs in the cloud. We have implemented our prototype in Python in about 2,000 lines of code, and currently support running VMs on the Google Cloud Platform [4].

We use a centralized controller (Figure 6), which implements the VM selection and job scheduling policies described in Section 4. The controller can run on any machine (including the user’s local machine, or inside a cloud VM), and exposes an HTTP API to end-users. Users submit either a bag or individual jobs to the controller via the HTTP API, which then launches and maintains a cluster of cloud VMs, and maintains the job queue and metadata in a local database.

SciSpot integrates, and interfaces with two primary services. First, it uses the Google cloud API [3] for launching, terminating, and monitoring VMs. Once a cluster is launched, it then configures a cluster manager such as Slurm [8] or Torque [10], to which it submits jobs. SciSpot uses the Slurm cluster manager, with each VM acting as a Slurm “cloud” node, which allows Slurm to gracefully handle VM preemptions. The Slurm master node runs on a small, 2 CPU non-preemptible VM, which is shared by all applications and users. We monitor job completions and failures (due to VM preemptions) through the use of Slurm call-backs, which issue HTTP requests back to the central service controller.

**Policy Implementation:** SciSpot creates and manages clusters of transient cloud servers, manages all aspects of the VM lifecycle and costs, and implements the model-based policies. It manages a cluster of VMs, and parametrizes the bathtub model based on the VM type, region, time-of-day, and day-of-week. When a new batch job is to be launched, we find a “free” VM in the cluster that is idle, and uses the job scheduling policy to determine if the VM is suitable or a new VM must be launched. Due to the bathtub nature of the failure rate, VMs that have survived the initial failures are “stable” and have a very low rate of failure, and thus are “valuable”. We keep these stable VMs as “hot spares” instead of terminating them, for a period of one hour.

**Bag of Jobs Abstraction For Scientific Simulations:** While SciSpot is intended for general batch jobs, we incorporate a special optimization for scientific simulation workloads that improves the ease-of-use of our service, and also helps in our policy implementation. We allow users to submit entire bags of jobs, which permits us to determine the running time of jobs based on previous jobs in the bag. For constrained preemptions, the running time and checkpointing are determined by job lengths, and the job run time estimates are extremely useful. Having a large sequence of jobs is also particularly useful with bathtub preemptions, since we can re-use “stable” VMs with low preemption probability for running new jobs from a bag. If jobs were submitted one at a time, a batch computing service may have to terminate the VM after job completion, which would increase the job failure probability resulting from running on new VMs that have a high initial failure rate.

## 6 SCI~~S~~OT EXPERIMENTAL EVALUATION

In this section, we present analytical and empirical evaluation of constrained preemptions. We have already presented the statistical analysis of our model in Section 3, and we now focus on answering the following questions:

- 1) How do constrained preemptions impact the total running time of applications?
- 2) What is the effect of our model-based policies when compared to existing transient computing approaches?
- 3) What is the cost and performance of SciSpot for real-world workloads?

**Environment and Workloads:** All our empirical evaluation is conducted on the Google Cloud Platform using our batch computing service described in Section 5. All the experiments are conducted in the same time period, and have the same preemption characteristics, as described in our data collection methodology in Section 3. We use three scientific computing workloads that are representative of applications in the broad domains of physics and material sciences:

**Nanoconfinement.** The nanoconfinement application launches molecular dynamics (MD) simulations of ions in nanoscale confinement created by material surfaces [40], [44]. The running time is 14 minutes on a 64 CPU core cluster (4 n1-highcpu-16 VMs).

**Shapes.** The Shapes application runs an MD-based optimization dynamics to predict the optimal shape of deformable, charged nanoparticles [37], [19], [42]. The running time is 9 minutes on a 64 CPU core cluster (4 n1-highcpu-16 VMs).

**LULESH.** Livermore Unstructured Lagrangian Explicit Shock Hydrodynamics is a popular benchmark for hydrodynamics simulations of continuum material models [46], [47]. The running time is 12.5 minutes on 8 n1-highcpu-8 VMs.

### 6.1 Model-based Policies

We now evaluate the effectiveness of model-driven policies that we proposed earlier in Section 4. Wherever applicable, we compare against policies designed for EC2 spot instances [33], [67] that have memoryless preemptions. However we also note that certain resource management challenges such as the preemption-rate aware job scheduling are *inherent* to constrained preemptions, and no existing equivalent policies can be found for memoryless techniques.

#### 6.1.1 Job Scheduling

Previously, we have quantified the increase in running time due to preemptions, but we had assumed that jobs start on a newly launched server. In many scenarios however, a server may be used for running a long-running sequence of jobs, such as in a batch-computing service. Our job scheduling policy is model-driven and decides whether to request a new VM for a job or run it on an existing VM. A new VM may be preferable if the job starts running near the VM’s 24 hour preemption deadline.

Figure 7 shows the effect of our job scheduling policy for a six hour job, for different job starting times (relative to the VM’s starting time). We compare against a baseline of memoryless job scheduling that is not informed by constrained preemption dynamics. Such memoryless policies are the default in existing transient computing systems such as SpotOn [67]. In the absence of insights about bathtub preemptions, the memoryless policy continues to run jobs on the existing VM. As the figure shows, the empirical job failure probability is bathtub shaped. However since the job is 6 hours long, with the memoryless policy, it will always fail when launched after  $24 - 6 = 18$  hours. In contrast, our model-based policy determines that after 18 hours, we will be better off running the job on a newer VM, and results in a constant lower job failure probability ( $=0.4$ ). The failure probability is constant because the jobs will always be launched on a new VM after 18 hours, resulting in a failure probability at time=0. Thus, our model-based job scheduling policy can reduce job failure probability by taking into account the time-varying failure rates of VMs, which is not considered by existing systems that use memoryless scheduling policies.

The job failure probability is determined by the job length and the job starting time. We examine the failure probability for jobs of different lengths (uniformly distributed) in Figure 8, in which we average the failure probability across different start times. We again see that our policy results in significantly lower failure probability compared to memoryless scheduling. For all but the shortest and longest jobs, the failure probability with our policy is *half* of that of existing memoryless policies. This reduction is primarily due to how the two policies perform for jobs launched near the end of the VM preemption deadline, which we examined previously in Figure 7.

**Sensitivity to model fitting.** The effectiveness of any model-based policy depends on the goodness of fit of the preemption model—i.e., how accurately it captures empirical data. We now evaluate the impact on our scheduling policy if incorrect/suboptimal model parameters are with high goodness-of-fit ( $r^2$ ) error are used. That is, we seek to understand how sensitive our policies are when the underlying preemption behavior does not match the model, which can occur due to changes in supply/demand, minor cloud policy changes, etc. Figure 9 compares the job failure probability with the optimal bathtub model that best fits the empirical data, and a suboptimal bathtub model intentionally chosen to have a bad fit. Specifically, the suboptimal case models the n1-highcpu-16 VMs for n1-highcpu-32 VMs, which from Figure 3a we can see are significantly different. However even with the suboptimal model, the

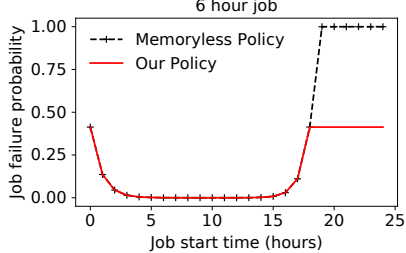


Fig. 7: Effect of job start time on the failure probability.

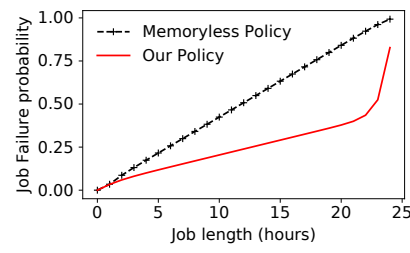


Fig. 8: Job failure probability for jobs of different lengths.

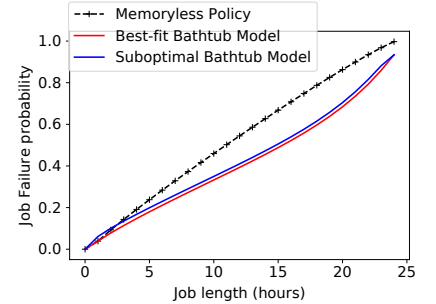


Fig. 9: Impact of suboptimal bathtub model parameters on the scheduling policy is negligible.

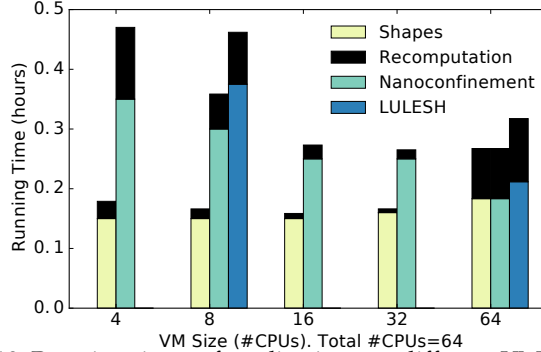


Fig. 10: Running times of applications on different VMs. Total number of CPUs is 64, yielding different number of VMs in each case. We see different tradeoffs in the base running times and recomputation times.

increase in job failure probability is less than 2% compared to the best-fit model. This negligible difference is due to the fact that even a suboptimal model captures the bathtub shape, and this is enough for the policy to make the “right” scheduling decision.

**Result:** Our policies are not particularly sensitive to the exact model parameters, so long as a bathtub distribution is used. Even a suboptimal bathtub model can reduce failure probability by 15% compared to the memoryless policy.

### 6.1.2 Impact of VM Selection

When an application (i.e., bag of jobs) requests a total number of CPUs to run each of its jobs, SciSpot first runs its exploration phase to find the “right” VM for the application. SciSpot searches for the VM that minimizes the total expected cost  $E[C_{(i,n_i)}]$  of running the application. Thus, even if the total amount of resources (i.e., number of CPUs) per job is held constant, the total running time (i.e., turnaround time) of an application depends on the choice of the VM type ( $i$ ), and the associated number of VMs ( $n_i$ ) required to meet the allocation constraint.

Figure 10 shows the running times of the Nanoconfinement, Shapes, and LULESH applications, when they are deployed on different VM sizes. In all cases, the total number of CPUs per job is set to 64, and thus the different VM sizes yield different cluster sizes (e.g., 16 VMs with 4 CPUs or 32 VMs with 2 CPUs). LULESH requires CPUs to be cube of an integer, which limits the valid cluster configurations.

For Nanoconfinement and LULESH, we observe that the base running times (without preemptions) reduce when moving to larger VMs, because this entails lower communication

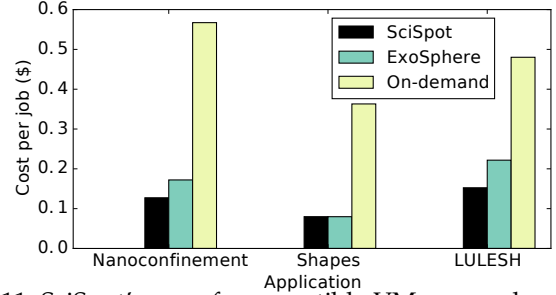


Fig. 11: SciSpot’s use of preemptible VMs can reduce costs by up to 5× compared to conventional cloud deployments, and 20% compared to the state of the art EC2 spot instance selection (ExoSphere [59]).

costs. For Nanoconfinement, the running time on the “best” VM (i.e., with 32 CPUs) is nearly 40% lower as compared to the worst case. On the other hand, the Shapes application can scale to a larger number of VMs without any significant communication overheads, and does not see any significant change in its running time.

Figure 10 also shows the expected recomputation time which depends on the expected lifetimes of the VM and the number of VMs. While selecting larger VMs may reduce communication overheads and thus improve performance, it is not an adequate policy in the case of preemptible VMs, since the preemptions can significantly increase the turnaround time. Therefore, even though the base running time of Nanoconfinement is lower on a 64 CPU VM, the recomputation time on the 64 CPU VM is almost 4× higher compared to a 2x32-CPU cluster, due to the much lower expected lifetime of the larger VMs. Thus, on preemptible servers, there is a tradeoff between the base running time which only considers parallelization overheads, and the recomputation time. By considering both these factors, SciSpot’s server selection policy can select the best VM for an application.

**Result:** SciSpot’s server selection, by considering both the base running time and recomputation time, can improve performance by up to 40%, and can keep the increase in running time due to preemptions to less than 5%.

### 6.1.3 Cost

The primary motivation for using preemptible VMs is their significantly lower cost compared to conventional “on-demand” cloud VMs that are non-preemptible. Figure 11 compares the cost of running different applications with different cloud VM deployments. SciSpot, which uses both

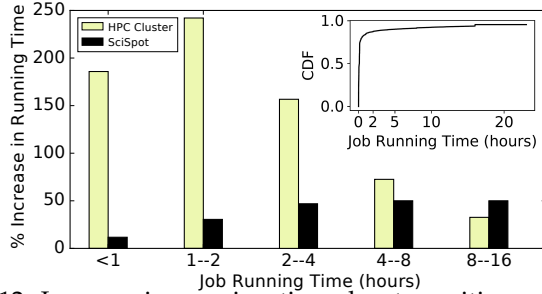


Fig. 12: Increase in running time due to waiting on HPC clusters is significantly higher than the recomputation time for SciSpot, except for very long and rare jobs (see inset).

cost-minimizing server selection, and preemptible VMs, results in significantly lower costs across the board, even when accounting for preemptions and recomputations. We also compare against ExoSphere [59], a state of the art system for transient server selection. ExoSphere implements a portfolio-theory approach using EC2 spot prices to balance average cost saving and risk of revocations using diversification and selecting VMs with low price correlation. However, this approach is ineffective for the flat prices of Google Preemptible VMs. Unlike SciSpot, ExoSphere does *not* consider application performance when selecting servers, and thus is unable to select the best server for parallel applications. Since the Google highcpu VMs have the same price per CPU, ExoSphere picks an arbitrary “median” VM to break ties, which may not necessarily yield the lowest running times. This results in 20% cost increase over SciSpot.

**Result:** *SciSpot reduces computing costs by up to 5× compared to conventional on-demand cloud deployments.*

#### 6.1.4 Comparison with HPC Overhead

Scientific computing applications are typically run on large-scale HPC clusters, where different performance and cost dynamics apply. While there are hardware differences between cloud VMs and HPC clusters that can contribute to performance differences, we are interested in the performance “overheads”. In the case of SciSpot, the job failures and recomputations increase the job turnaround time, and are thus the main source of overhead.

On HPC clusters, jobs enjoy significantly lower recomputation probability, since the hardware on these clusters has MTTFs in the range of years to centuries [26]. However, we emphasize that there exist *other* sources of performance overheads in HPC clusters. In particular, since HPC clusters have high resource utilization, they also have significant *waiting* times. On the other hand, cloud resource utilization is low [73] and there is usually no need to wait for resources, which is why transient servers exist in the first place.

Thus, we compare the performance overhead due to preemptions for SciSpot, and job waiting times in conventional HPC deployments. To obtain the job waiting times in HPC clusters, we use the LANL Mustang traces published as part of the Atlas trace repository [12]. We analyze the waiting time of over two million jobs submitted over a 5 year period, and compute the increase in running time of the job due to the job waiting or queuing time.

Figure 12 compares the overhead (as percentage increase in running time) of SciSpot and HPC clusters for jobs of

different lengths. We see that the average performance overhead due to waiting can be significant in the case of HPC clusters, and the job submission latency and queuing time dominate for smaller jobs, increasing their total turnaround time by more 2.5×. This waiting is amortized in the case of longer running jobs, and the overhead for longer jobs is around 30%.

On the other hand, SciSpot’s performance overhead is significantly smaller for jobs of up to 8 hours in length. For longer jobs, the limited lifetime of Google Preemptible VMs (24 hours) begins to significantly increase the preemption probability and expected recomputation time. We emphasize that these are *individual* job lengths, and not the running time of entire bag of jobs. We note that these large single jobs are rare, accounting for less than 5% of all HPC jobs (see inset in Figure 12). For smaller jobs (within a much larger bag), both the preemption probability and recomputation overhead is much smaller.

**Result:** *SciSpot’s overhead of recomputation due to preemptions is small, and is up to 10× lower compared to the overhead of waiting in conventional HPC clusters.*

## 7 RELATED WORK

**Transient Cloud Computing.** The significantly lower cost of spot instances makes them attractive for running preemption and delay tolerant batch jobs [67], [38], [81], [76], [50], [21], [27], [72], [33]. The challenges posed by Amazon EC2 spot instances, the first transient cloud servers, have received significant attention from both academia and industry [9]. The distinguishing characteristic of EC2 spot instances is their dynamic auction-based pricing, and choosing the “right” bid price to minimize cost and performance degradation is the focus of much of the past work on transient computing [39], [52], [70], [75], [80], [84], [82], [85], [66], [78], [32]. However, it remains to be seen how Amazon’s recent change [11], [35], [15], [55] in the preemption model of spot instances affects prior work. Non-price based transient availability models, such as temporally constrained preemptions, have received scant attention due to the difficulty in obtaining empirical preemption data—which we hope our dataset remedies.

**Preemption Mitigation.** Effective use of transient servers usually entails the use of fault-tolerance techniques such as checkpointing [57], migration [60], and replication [67]. In the context of HPC workloads, [51], [31], [69] develop checkpointing and bidding strategies for MPI applications running on EC2 spot instances. However, periodic checkpointing [26], [18] is not optimal in our case because preemptions are not memoryless.

**Preemption Modeling.** Conventionally, exponential distribution have been used to model preemptions, even for EC2 spot instances [85], [57], [58]. Our preemption model provides a novel characterization of bathtub shaped failure rates not captured even by Weibull distributions, and is distinct from prior efforts [53], [24]. Recent work [63] has also found evidence of the bath-tub failure distribution for Google Preemptible GPU VMs, and confirms our observations.

## REFERENCES

- [1] Alibaba Cloud Preemptible Instances. <https://www.alibabacloud.com/help/doc-detail/52088.htm>.

- [2] Amazon EC2 Spot Instances, howpublished=<https://aws.amazon.com/ec2/spot/>.
- [3] Google Cloud API Documentation. <https://cloud.google.com/apis/docs/overview>.
- [4] Google Cloud Platform. <https://cloud.google.com/>.
- [5] Google Cloud Preemptible VM Instances Documentation, howpublished=<https://cloud.google.com/compute/docs/instances/preemptible>.
- [6] Packet Spot Market. <https://support.packet.com/kb/articles/spot-market>.
- [7] Scipy curve fit documentation. [https://docs.scipy.org/doc/scipy/reference/generated/scipy.optimize.curve\\_fit.html](https://docs.scipy.org/doc/scipy/reference/generated/scipy.optimize.curve_fit.html).
- [8] Slurm Workload Manager. <https://slurm.schedmd.com/documentation.html>.
- [9] Spotinst. <https://spotinst.com/>.
- [10] Torque Resource Manager. <http://www.adaptivecomputing.com/products/torque>.
- [11] New Amazon EC2 Spot pricing model. <https://aws.amazon.com/blogs/compute/new-amazon-ec2-spot-pricing/>, March 2018.
- [12] AMVROSIADIS, G., PARK, J. W., GANGER, G. R., GIBSON, G. A., BASEMAN, E., AND DEBARDELEBEN, N. On the diversity of cluster workloads and its impact on research results. In *2018 {USENIX} Annual Technical Conference ({USENIX} {ATC} 18)* (2018), pp. 533–546.
- [13] Azure Low-priority Batch VMs. <https://docs.microsoft.com/en-us/azure/batch/batch-low-pri-vms>.
- [14] BARTÓK, A. P., DE, S., POELKING, C., BERNSTEIN, N., KERMODE, J. R., CSÁNYI, G., AND CERIOTTI, M. Machine learning unifies the modeling of materials and molecules. *Science Advances* 3, 12 (2017).
- [15] BAUGHMAN, M., CATON, S., HAAS, C., CHARD, R., WOLSKI, R., FOSTER, I., AND CHARD, K. Deconstructing the 2017 changes to aws spot market pricing. In *Proceedings of the 10th Workshop on Scientific Cloud Computing* (2019), ACM, pp. 19–26.
- [16] BAUGHMAN, M., HAAS, C., WOLSKI, R., FOSTER, I., AND CHARD, K. Predicting amazon spot prices with lstm networks. In *Proceedings of the 9th Workshop on Scientific Cloud Computing* (2018), ACM, p. 1.
- [17] BEN-YEHUDA, O., BEN-YEHUDA, M., SCHUSTER, A., AND TSAFRIR, D. Deconstructing Amazon EC2 Spot Instance Pricing. *ACM TEC* 1, 3 (September 2013).
- [18] BOUGERET, M., CASANOVA, H., RABIE, M., ROBERT, Y., AND VIVIEN, F. Checkpointing strategies for parallel jobs. In *Proceedings of 2011 International Conference for High Performance Computing, Networking, Storage and Analysis on - SC '11* (Seattle, Washington, 2011), ACM Press, p. 1.
- [19] BRUNK, N. E., AND JADHAO, V. Computational studies of shape control of charged deformable nanocontainers. *Journal of Materials Chemistry B* 7 (2019), 6370.
- [20] CH'NG, K., CARRASQUILLA, J., MELKO, R. G., AND KHATAMI, E. Machine learning phases of strongly correlated fermions. *Phys. Rev. X* 7 (Aug 2017), 031038.
- [21] CHOCHAN, N., CASTILLO, C., SPREITZER, M., STEINDER, M., TANTAWI, A., AND KRINTZ, C. See Spot Run: Using Spot Instances for MapReduce Workflows. In *HotCloud* (June 2010).
- [22] CIRNE, W., BRASILEIRO, F., SAUVE, J., ANDRADE, N., PARANHOS, D., SANTOS-NETO, E., AND MEDEIROS, R. Grid computing for bag of tasks applications. In *In Proc. of the 3rd IFIP Conference on E-Commerce, E-Business and EGovernment* (2003), IFIP.
- [23] CORTEZ, E., BONDE, A., MUZIO, A., RUSSINOVICH, M., FONTOURA, M., AND BIANCHINI, R. Resource central: Understanding and predicting workloads for improved resource management in large cloud platforms. In *Proceedings of the 26th Symposium on Operating Systems Principles* (New York, NY, USA, 2017), SOSP '17, ACM, pp. 153–167.
- [24] CREVECOEUR, G. A model for the integrity assessment of ageing repairable systems. *IEEE Transactions on reliability* 42, 1 (1993), 148–155.
- [25] DALY, J. T. A Higher Order Estimate of the Optimum Checkpoint Interval for Restart Dumps. *Future Generation Computer Systems* 22, 3 (2006).
- [26] DONGARRA, J., HERAULT, T., AND ROBERT, Y. Fault tolerance techniques for high-performance computing. 66.
- [27] DUBOIS, D. J., AND CASALE, G. Optispot: minimizing application deployment cost using spot cloud resources. *Cluster Computing* (2016), 1–17.
- [28] FERGUSON, A. L. Machine learning and data science in soft materials engineering. *Journal of Physics: Condensed Matter* 30, 4 (2017), 043002.
- [29] FOX, G., GLAZIER, J. A., KADUPITIYA, J., JADHAO, V., KIM, M., QIU, J., SLUKA, J. P., SOMOGYI, E., MARATHE, M., ADIGA, A., ET AL. Learning Everywhere: Pervasive machine learning for effective High-Performance computation. *arXiv preprint arXiv:1902.10810* (2019).
- [30] GHIT, B., AND EPEMA, D. Better safe than sorry: Grappling with failures of in-memory data analytics frameworks. In *Proceedings of the 26th International Symposium on High-Performance Parallel and Distributed Computing* (New York, NY, USA, 2017), HPDC '17, ACM, pp. 105–116.
- [31] GONG, Y., HE, B., AND ZHOU, A. C. Monetary cost optimizations for MPI-based HPC applications on Amazon clouds: checkpoints and replicated execution. In *Proceedings of the International Conference for High Performance Computing, Networking, Storage and Analysis on - SC '15* (Austin, Texas, 2015), ACM Press, pp. 1–12.
- [32] GUO, W., CHEN, K., WU, Y., AND ZHENG, W. Bidding for Highly Available Services with Low Price in Spot Instance Market. In *Proceedings of the 24th International Symposium on High-Performance Parallel and Distributed Computing - HPDC '15* (Portland, Oregon, USA, 2015), ACM Press, pp. 191–202.
- [33] HARLAP, A., CHUNG, A., TUMANOV, A., GANGER, G. R., AND GIBBONS, P. B. Tributary: spot-dancing for elastic services with latency slos. In *2018 {USENIX} Annual Technical Conference ({USENIX} {ATC} 18)* (2018), pp. 1–14.
- [34] HARLAP, A., TUMANOV, A., CHUNG, A., GANGER, G. R., AND GIBBONS, P. B. Proteus: Agile ml elasticity through tiered reliability in dynamic resource markets. In *Proceedings of the Twelfth European Conference on Computer Systems* (New York, NY, USA, 2017), EuroSys '17, ACM, pp. 589–604.
- [35] IRWIN, D., SHENOY, P., AMBATI, P., SHARMA, P., SHASTRI, S., AND ALI-ELDIN, A. The price is (not) right: Reflections on pricing for transient cloud servers. *2019 28th International Conference on Computer Communication and Networks (ICCCN)* (2019), 1–9.
- [36] JADHAO, V., AND ROBBINS, M. O. Rheological properties of liquids under conditions of elastohydrodynamic lubrication. *Tribology Letters* 67, 3 (2019), 66.
- [37] JADHAO, V., THOMAS, C. K., AND OLVERA DE LA CRUZ, M. Electrostatics-driven shape transitions in soft shells. *Proceedings of the National Academy of Sciences* 111, 35 (2014), 12673–12678.
- [38] JAIN, N., MENACHE, I., AND SHAMIR, O. On-demand, spot, or both: Dynamic resource allocation for executing batch jobs in the cloud. In *11th International Conference on Autonomic Computing (ICAC 14)*, USENIX Association.
- [39] JAVADI, B., THULASIRAM, R., AND BUYYA, R. Statistical Modeling of Spot Instance Prices in Public Cloud Environments. In *UCC* (December 2011).
- [40] JING, Y., JADHAO, V., ZWANIKKEN, J. W., AND OLVERA DE LA CRUZ, M. Ionic structure in liquids confined by dielectric interfaces. *The Journal of chemical physics* 143, 19 (2015), 194508.
- [41] JOAQUIM, P., BRAVO, M., RODRIGUES, L., AND MATOS, M. Hourglass: Leveraging transient resources for time-constrained graph processing in the cloud. In *Proceedings of the Fourteenth EuroSys Conference 2019* (New York, NY, USA, 2019), EuroSys '19, ACM, pp. 35:1–35:16.
- [42] KADUPITIYA, J., BRUNK, N., AND JADHAO, V. Nanoparticle shape lab, January 2020. nanoHUB.
- [43] KADUPITIYA, J., FOX, G. C., AND JADHAO, V. Machine learning for performance enhancement of molecular dynamics simulations. In *International Conference on Computational Science* (2019), pp. 116–130.
- [44] KADUPITIYA, J., MARRU, S., FOX, G. C., AND JADHAO, V. Ions in nanoconfinement, Dec 2017. Online on nanoHUB; source code on GitHub at [github.com/softmaterialslab/nanoconfinement-md](https://github.com/softmaterialslab/nanoconfinement-md).
- [45] KADUPITIYA, J., SUN, F., FOX, G., AND JADHAO, V. Machine learning surrogates for molecular dynamics simulations of soft materials. *Journal of Computational Science* (2020), 101107.
- [46] KARLIN, I., BHATELE, A., KEASLER, J., CHAMBERLAIN, B. L., COHEN, J., DEVITO, Z., HAQUE, R., LANEY, D., LUKE, E., WANG, F., RICHARDS, D., SCHULZ, M., AND STILL, C. Exploring traditional and emerging parallel programming models using a proxy application. In *27th IEEE International Parallel & Distributed Processing Symposium (IEEE IPDPS 2013)* (Boston, USA, May 2013).
- [47] KARLIN, I., KEASLER, J., AND NEELY, R. Lulesh 2.0 updates and changes. Tech. Rep. LLNL-TR-641973, August 2013.
- [48] KLOTSA, D., CHEN, E. R., ENGEL, M., AND GLOTZER, S. C. Intermediate crystalline structures of colloids in shape space. *Soft Matter* 14, 43 (2018), 8692–8697.

- [49] KRAUTH, W. *Statistical mechanics: algorithms and computations*, vol. 13. OUP Oxford, 2006.
- [50] LIU, H. Cutting MapReduce Cost with Spot Market. In *HotCloud* (June 2011).
- [51] MARATHE, A., HARRIS, R., LOWENTHAL, D., DE SUPINSKI, B. R., ROUNTREE, B., AND SCHULZ, M. Exploiting redundancy for cost-effective, time-constrained execution of hpc applications on amazon ec2. In *HPDC* (2014), ACM.
- [52] MIHAILESCU, M., AND TEO, Y. M. The Impact of User Rationality in Federated Clouds. In *CCGrid* (2012).
- [53] MUDHOLKAR, G. S., AND SRIVASTAVA, D. K. Exponentiated weibull family for analyzing bathtub failure-rate data. *IEEE transactions on reliability* 42, 2 (1993), 299–302.
- [54] OUYANG, X., IRWIN, D., AND SHENOY, P. Spotlight: An information service for the cloud. In *IEEE International Conference on Distributed Computing Systems (ICDCS)* (2016).
- [55] PHAM, T.-P., RISTOV, S., AND FAHRINGER, T. Performance and behavior characterization of amazon ec2 spot instances. In *2018 IEEE 11th International Conference on Cloud Computing (CLOUD)* (2018), IEEE, pp. 73–81.
- [56] SCHOENHOLZ, S. S. Combining machine learning and physics to understand glassy systems. *Journal of Physics: Conference Series* 1036, 1 (2018), 012021.
- [57] SHARMA, P., GUO, T., HE, X., IRWIN, D., AND SHENOY, P. Flint: Batch-Interactive Data-Intensive Processing on Transient Servers. In *EuroSys* (April 2016).
- [58] SHARMA, P., IRWIN, D., AND SHENOY, P. How Not to Bid the Cloud. In *Proceedings of the 8th USENIX Workshop on Hot Topics in Cloud Computing (HotCloud)* (June 2016), USENIX.
- [59] SHARMA, P., IRWIN, D., AND SHENOY, P. Portfolio-driven resource management for transient cloud servers. In *Proceedings of ACM Measurement and Analysis of Computer Systems* (June 2017), vol. 1, p. 23.
- [60] SHARMA, P., LEE, S., GUO, T., IRWIN, D., AND SHENOY, P. SpotCheck: Designing a Derivative IaaS Cloud on the Spot Market. In *EuroSys* (April 2015).
- [61] SHAstri, S., AND IRWIN, D. Hotspot: automated server hopping in cloud spot markets. In *Proceedings of the 2017 Symposium on Cloud Computing* (2017), ACM, pp. 493–505.
- [62] SHAstri, S., RIZK, A., AND IRWIN, D. Transient guarantees: Maximizing the value of idle cloud capacity. In *Proceedings of the International Conference for High Performance Computing, Networking, Storage and Analysis* (Piscataway, NJ, USA, 2016), SC ’16, IEEE Press, pp. 85:1–85:11.
- [63] SHIJIAN LI, R. W., AND GUO, T. Characterizing and modeling distributed training with transient cloud gpu servers. *40th IEEE International Conference on Distributed Computing Systems (ICDCS’20)*.
- [64] SINGH, R., SHARMA, P., IRWIN, D., SHENOY, P., AND RAMAKRISHNAN, K. Here Today, Gone Tomorrow: Exploiting Transient Servers in Data Centers. *IEEE Internet Computing* 18, 4 (July/August 2014).
- [65] SOLIS, F. J., JADHAO, V., AND DE LA CRUZ, M. O. Generating true minima in constrained variational formulations via modified lagrange multipliers. *Physical Review E* 88, 5 (2013), 053306.
- [66] SONG, Y., ZAFER, M., AND LEE, K. Optimal Bidding in Spot Instance Market. In *Infocom* (March 2012).
- [67] SUBRAMANYA, S., GUO, T., SHARMA, P., IRWIN, D., AND SHENOY, P. SpotOn: A Batch Computing Service for the Spot Market. In *SOCC* (August 2015).
- [68] SUN, Y., DEJACO, R. F., AND SIEPMANN, J. I. Deep neural network learning of complex binary sorption equilibria from molecular simulation data. *Chemical science* 10, 16 (2019), 4377–4388.
- [69] TAIFI, M., SHI, J. Y., AND KHREISHAH, A. SpotMPI: A Framework for Auction-Based HPC Computing Using Amazon Spot Instances. In *Algorithms and Architectures for Parallel Processing*, Y. Xiang, A. Cuzzocrea, M. Hobbs, and W. Zhou, Eds., vol. 7017. Springer Berlin Heidelberg, Berlin, Heidelberg, 2011, pp. 109–120.
- [70] TANG, S., YUAN, J., AND LI, X. Towards Optimal Bidding Strategy for Amazon EC2 Cloud Spot Instance. In *CLOUD* (June 2012).
- [71] TONKS, L. The complete equation of state of one, two and three-dimensional gases of hard elastic spheres. *Phys. Rev.* 50 (Nov 1936), 955–963.
- [72] VARSHNEY, P., AND SIMMHAN, Y. AutoBoT : Resilient and Cost-effective Scheduling of a Bag of Tasks on Spot VMs. *IEEE Transactions on Parallel and Distributed Systems* (2019), 1–1.
- [73] VERMA, A., PEDROSA, L., KORUPOLU, M., OPPENHEIMER, D., TUNE, E., AND WILKES, J. Large-scale cluster management at google with borg. In *EuroSys* (2015), ACM.
- [74] WANG, J., OLSSON, S., WEHMEYER, C., PEREZ, A., CHARRON, N. E., DE FABRITIIS, G., NOE, F., AND CLEMENTI, C. Machine learning of coarse-grained molecular dynamics force fields. *ACS central science* (2019).
- [75] WEE, S. Debunking Real-Time Pricing in Cloud Computing. In *CCGrid* (May 2011).
- [76] WIEDER, A., BHATOTIA, P., POST, A., AND RODRIGUES, R. Orchestrating the deployment of computations in the cloud with conductor. In *NSDI 12* (2012).
- [77] WOLSKI, R., AND BREVIK, J. Providing statistical reliability guarantees in the aws spot tier. In *Proceedings of the 24th High Performance Computing Symposium* (2016), Society for Computer Simulation International, p. 13.
- [78] WOLSKI, R., BREVIK, J., CHARD, R., AND CHARD, K. Probabilistic guarantees of execution duration for Amazon spot instances. In *Proceedings of the International Conference for High Performance Computing, Networking, Storage and Analysis on - SC ’17* (Denver, Colorado, 2017), ACM Press, pp. 1–11.
- [79] WOLSKI, R., BREVIK, J., CHARD, R., AND CHARD, K. Probabilistic guarantees of execution duration for amazon spot instances. In *Proceedings of the International Conference for High Performance Computing, Networking, Storage and Analysis* (2017), ACM, p. 18.
- [80] XU, H., AND LI, B. A Study of Pricing for Cloud Resources. *Performance Evaluation Review* 40, 4 (March 2013).
- [81] YI, S., KONDO, D., AND ANDRZEJAK, A. Reducing costs of spot instances via checkpointing in the amazon elastic compute cloud. In *Cloud Computing (CLOUD), 2010 IEEE 3rd International Conference on* (2010), IEEE, pp. 236–243.
- [82] ZAFER, M., SONG, Y., AND LEE, K. Optimal Bids for Spot VMs in a Cloud for Deadline Constrained Jobs. In *CLOUD* (2012).
- [83] ZHANG, C., GUPTA, V., AND CHIEN, A. A. Information models: Creating and preserving value in volatile cloud resources. In *2019 IEEE International Conference on Cloud Engineering (IC2E)* (June 2019), pp. 45–55.
- [84] ZHANG, Q., GÜRSes, E., BOUTABA, R., AND XIAO, J. Dynamic Resource Allocation for Spot Markets in Clouds. In *Hot-ICE* (March 2011).
- [85] ZHENG, L., JOE-WONG, C., TAN, C. W., CHIANG, M., AND WANG, X. How to Bid the Cloud. In *SIGCOMM* (August 2015).